JOURNAL OF GUIDANCE, CONTROL, AND DYNAMICS
Vol. 22, No. 6, November–December 1999

Robust Stability of Mode-to-Mode Fuzzy Controllers

Freeman Rufus* and George Vachtsevanos†
Georgia Institute of Technology, Atlanta, Georgia 30332-0250

An approximate method is formulated for analyzing the performance of nonlinear systems controlled by mode-to-mode fuzzy controllers. It is assumed that an approximate model of the nominal plant is available and the nominal mode-to-mode trajectory converges asymptotically from the start mode to the target mode of operation. Stability of the nominal mode-to-mode trajectory in the presence of small, bounded variations of the system's parameters or the initial conditions is considered. The method is based on formulating a performance measure as a Lyapunov function of the error between the nominal and perturbed mode-to-mode trajectories. The sensitivity of the deviations from the nominal mode-to-mode trajectory with respect to parametric or initial condition variations is incorporated into the total differential of this performance measure. Using a Lyapunov stability condition, the robustness of the closed-loop system is analyzed by observing a definiteness condition of a time-varying matrix. A measure of robustness is then formulated using the largest singular value of a time-varying matrix. A hover mode to forward flight mode fuzzy controller is used to illustrate the methodology.

I. Introduction

ALTHOUGH an often-mentioned reason for using fuzzy logic controllers is the lack of an accurate system model, the availability of an approximate dynamical model of the plant has not been fully explained when addressing issues of robust performance in the design of such control strategies. In Refs. 1 and 2, an attempt was made to bridge the gap between precise performance specifications and the use of fuzzy logic controllers along with an approximate dynamical model of the plant to be controlled. This attempt involved formulating a performance measure as a Lyapunov-like function of the error dynamics of the nominal plant. This performance measure also incorporated a heuristic measure of the system's error sensitivity with respect to parametric variations. The robust stability addressed in this context was stability convergence to an equilibrium point in the presence of small parametric perturbations. Inequality bounds were derived for the sensitivity, error deviation, and parameter deviations in terms of fuzzy quantities. Finally, a measure of robustness was formulated using singular values. This methodology was used to analyze the robustness of an automotive engine idle speed fuzzy controller.[1]

In this paper, the formulation in Refs. 1 and 2 is extended to study the robust stability of the nominal trajectory of a mode-to-mode fuzzy controller where the trajectory is considered to be feasible (or realistic). Given a nominal mode-to-mode trajectory that converges asymptotically from the equilibrium point of the start mode to the equilibrium point of the target mode of operation, the stability of this nominal trajectory, in the presence of variations of the system's parameters or initial conditions, inherently addresses the robust stability of the closed-loop system. The robust stability of the nominal mode-to-mode trajectory is considered because perturbed trajectories that remain close to the nominal trajectory will also transition from the start mode to a small neighborhood around the equilibrium point of the target mode. Because the robust stability of the nominal trajectory is considered, the performance measure is formulated as a Lyapunov function of the error between the nominal and perturbed trajectories. The total differential of this performance measure also incorporates the sensitivity of the trajectory error with respect to parametric or initial condition variations. The robustness of the closed-loop system is analyzed by observing a definiteness condition of a time-varying matrix. A measure of robustness is then formulated using the infinity norm of a time-varying matrix. Finally, a hover mode to forward flight (FF) mode controller is used to illustrate the methodology.

II. Robust Stability Analysis of Mode-to-Mode Controllers

A. Introduction to Mode-to-Mode Transition Problem

Statement of Problem

A large-scale dynamic interconnected system is represented by the following state equation:

$$\dot{\boldsymbol{x}} = \boldsymbol{F}(\boldsymbol{x}, \boldsymbol{u}, t), \qquad \boldsymbol{x}(t_0) = \boldsymbol{x}_0, \qquad \boldsymbol{x} \in R^n, \quad \boldsymbol{u} \in R^m$$

It is assumed that the system can be decomposed into N interconnected subsystems $S_i, i = 1, 2, \ldots, N$, where each subsystem represents the modes of operation and the ith subsystem's state equation is

$$\dot{\boldsymbol{x}}_i = \boldsymbol{f}_i(\boldsymbol{x}_i, \boldsymbol{u}_i, t) + \sum_{\substack{j=1 \\ i \neq j}}^{N} \boldsymbol{g}_{ij}(\boldsymbol{x}_j, t), \qquad \boldsymbol{x}_i(t_0) = \boldsymbol{x}_i^0$$

$$\boldsymbol{x}_j \in R^{n_j}, \quad \boldsymbol{u}_j \in R^{m_j}, \quad \boldsymbol{g}_{ij}(\boldsymbol{x}_j, t) \in R^{n_i}$$

where $\boldsymbol{g}_{ij}(\boldsymbol{x}_j, t)$ represents the coupling term because of the jth subsystem. How do we design a hierarchical controller that stabilizes each mode of operation locally and is able to transition between modes stably?

Approach

Although this paper will present robust stability results using a mode-to-mode controller designed via the phase portrait assignment algorithm (PPAA), there are many alternate techniques available to smooth control transition from one mode to another. For example, given a specified mode-to-mode trajectory, piecewise smooth controls can be determined such that the error between the system output vector and the specified trajectory is minimized in the least-squares sense.[3] If a specified trajectory is not given, then piecewise smooth controls can be determined using nonlinear programming techniques such that the resultant mode-to-mode trajectory satisfy some smoothness criteria.[4]

Let mode$_p$ and mode$_q$ denote the pth and the qth subsystem modes, respectively. Using the PPAA, a mode$_p$-to-mode$_q$ transitional controller is designed with knowledge about the states of mode$_p$ and mode$_q$, and the outputs of the mode$_p$ and mode$_q$ controllers. The outputs of the mode$_p$-to-mode$_q$ controller are determined by blending the outputs of the mode$_p$ and mode$_q$ controllers. The blending weights for each mode controller are determined by the PPAA. A detailed description of the PPAA and its fuzzy hypercube implementation platform may be found in Refs. 5–7. The following is an outline for the design of the mode$_p$-to-mode$_q$ controller.

Received 27 August 1998; revision received 15 February 1999; accepted for publication 20 March 1999.

*Graduate Research Assistant, Intelligent Controls Laboratory, School of Electrical and Computer Engineering.

†Professor, Intelligent Controls Laboratory, School of Electrical and Computer Engineering; george.vachtsevanos@ee.gatech.edu.

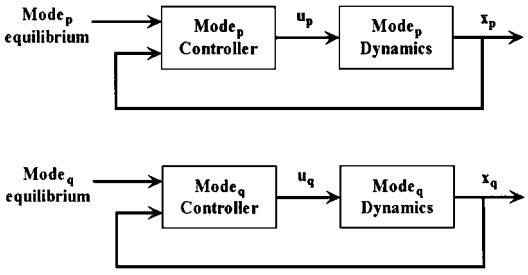

Fig. 1 Block diagram of mode$_p$ and mode$_q$ feedback systems.

1) Design local controllers for mode$_p$ and mode$_q$. For the operating modes mode$_p$ and mode$_q$, models are constructed that capture their local dynamics. Afterward linear or nonlinear state feedback controllers are designed for the two operating modes. The controllers are designed to regulate initial states belonging to mode$_p$ and mode$_q$ to the equilibrium point of mode$_p$ and mode$_q$, respectively. Figure 1 shows the feedback structure of the mode controllers, where the equilibrium point of mode$_p$ and mode$_q$ is the desired command.

The dynamical equations of mode$_p$ and mode$_q$, respectively, may be written as

$$\dot{\boldsymbol{x}}_p = \boldsymbol{f}_p(\boldsymbol{x}_p, \boldsymbol{u}_p), \qquad \boldsymbol{x}_p(t_0) = \boldsymbol{x}_p^0, \qquad \boldsymbol{x}_p \in R^{n_p}, \quad \boldsymbol{u}_p \in R^{m_p}$$
$$\boldsymbol{u}_p = \boldsymbol{\varphi}_p\left(\boldsymbol{x}_p - \boldsymbol{x}_p^*\right)$$
$$\dot{\boldsymbol{x}}_q = \boldsymbol{f}_q(\boldsymbol{x}_q, \boldsymbol{u}_q), \qquad \boldsymbol{x}_q(t_0) = \boldsymbol{x}_q^0, \qquad \boldsymbol{x}_q \in R^{n_q}, \quad \boldsymbol{u}_q \in R^{m_q}$$
$$\boldsymbol{u}_q = \boldsymbol{\varphi}_q\left(\boldsymbol{x}_q - \boldsymbol{x}_q^*\right)$$

where $\boldsymbol{x}_p^*$ and $\boldsymbol{x}_q^*$ denote the equilibrium points of mode$_p$ and mode$_q$, respectively; $\boldsymbol{\varphi}_p$ and $\boldsymbol{\varphi}_q$ are linear or nonlinear functions of $\boldsymbol{x}_p$ and $\boldsymbol{x}_q$.

2) Model combined dynamics of mode$_p$ and mode$_q$. A model of the dynamical system is constructed that incorporates the dynamics of mode$_p$, mode$_q$, and their corresponding coupling dynamics:

$$\dot{\boldsymbol{x}}_{pq} = \boldsymbol{f}(\boldsymbol{x}_{pq}, \boldsymbol{u}_{pq}), \qquad \boldsymbol{x}_{pq}(t_0) = \boldsymbol{x}_{pq}^0$$
$$\boldsymbol{x}_{pq} \in R^{n_{pq}}, \quad \boldsymbol{u}_{pq} \in R^{m_{pq}}$$

where $\boldsymbol{x}_{pq}$ is the vector of distinct elements of $[\boldsymbol{x}_p^T \ \boldsymbol{x}_q^T]^T$; $\boldsymbol{u}_{pq}$ is the vector of distinct elements of $[\boldsymbol{u}_p^T \ \boldsymbol{u}_q^T]^T$; $\boldsymbol{x}_p$ and $\boldsymbol{x}_q$ denote the states of mode$_p$ and mode$_q$, respectively; and $\boldsymbol{u}_p$ and $\boldsymbol{u}_q$ denote the control inputs of mode$_p$ and mode$_q$, respectively. Given the local models of mode$_p$ and mode$_q$, determining a model of the combined dynamics of mode$_p$ and mode$_q$ is really a problem of modeling the coupling terms: $\boldsymbol{g}_{pq}(\boldsymbol{x}_q) \in R^{n_p}$ and $\boldsymbol{g}_{qp}(\boldsymbol{x}_p) \in R^{n_q}$. The coupling dynamics can be modeled by invoking first principles or produced through experimental data. In the latter case, neural network, fuzzy or neurofuzzy models can be constructed.

3) Determine the region of interest and the partition of the $\boldsymbol{x}_{pq}$ phase space. A region of interest of the phase space belonging to $\boldsymbol{x}_{pq}$ is chosen such that it contains the operating points of mode$_p$, mode$_q$, and any corresponding transitional paths between the two modes, if they exist. Constraints on $\boldsymbol{x}_{pq}$ can be used to determine the maximum region of interest. Choosing a large region of interest will generally result in more partitions for each state of $\boldsymbol{x}_{pq}$ to meet a desired cell resolution; and more partitions for each state of $\boldsymbol{x}_{pq}$ will lead to more cells in the phase space, which will lead to a longer time to perform the phase space simulation. However, choosing a small region of interest increases the chance of excluding possible paths between mode$_p$ and mode$_q$. Therefore, the region of interest should be determined on the basis of the system's dynamics. The region of interest of the phase space is described by the following inequality:

$$(\boldsymbol{x}_{pq,\min})_i < (\boldsymbol{x}_{pq})_i < (\boldsymbol{x}_{pq,\max})_i, \qquad \text{for} \qquad i = 1, \ldots, n_p$$

where $(\boldsymbol{x}_{pq})_i$ is the ith state of $\boldsymbol{x}_{pq}$; $(\boldsymbol{x}_{pq,\min})_i$ and $(\boldsymbol{x}_{pq,\max})_i$ denote the minimum and maximum values of $(\boldsymbol{x}_{pq})_i$, respectively. The phase space is partitioned to have a desired cell resolution such that a tolerance specification is met and the equilibrium points of mode$_p$ and mode$_q$ are in different cells near the center of their respective cells. The number of cells in the region of interest of $\boldsymbol{x}_{pq}$ is

$$\prod_{i=1}^{n_{pq}} N_i$$

4) Determine the region of interest and partition of the blending weights phase space. Assuming the outputs of the mode$_p$ and mode$_q$ controllers are linearly blended, the mode$_p$-to-mode$_q$ controller $\boldsymbol{C}_{pq}$ will have the following form:

$$\boldsymbol{C}_{pq}(\cdot) = \boldsymbol{K}_p(\boldsymbol{x}_{pq}) \cdot \boldsymbol{u}_p + \boldsymbol{K}_q(\boldsymbol{x}_{pq}) \cdot \boldsymbol{u}_q$$

where $\boldsymbol{K}_p(\boldsymbol{x}_{pq})$ and $\boldsymbol{K}_q(\boldsymbol{x}_{pq})$ are the blending matrices; $\dim(\boldsymbol{K}_p(\boldsymbol{x}_{pq})) = m_{pq} \times m_p$ and $\dim(\boldsymbol{K}_q(\boldsymbol{x}_{pq})) = m_{pq} \times m_q$; m_p elements of $\boldsymbol{K}_p(\boldsymbol{x}_{pq})$ are nonzero; and m_q elements of $\boldsymbol{K}_q(\boldsymbol{x}_{pq})$ are nonzero. Let $k^{p1}, k^{p2}, \ldots, k^{pm_p}$ and $k^{q1}, k^{q2}, \ldots, k^{qm_q}$ denote the nonzero elements of $\boldsymbol{K}_p(\boldsymbol{x}_{pq})$ and $\boldsymbol{K}_q(\boldsymbol{x}_{pq})$, respectively. These nonzero elements of $\boldsymbol{K}_p(\boldsymbol{x}_{pq})$ and $\boldsymbol{K}_q(\boldsymbol{x}_{pq})$ are partitioned into admissible control inputs having the following ranges:

$$k_{\min}^{pr} \le k^{pr} \le k_{\max}^{pr}, \qquad \text{for} \qquad r = 1, \ldots, m_p$$
$$k_{\min}^{qr} \le k^{qr} \le k_{\max}^{qr}, \qquad \text{for} \qquad r = 1, \ldots, m_q$$

satisfying the following conditions:

a) If $(\boldsymbol{u}_{pq})_i$ is a control input belonging only to mode$_p$ then

$$(\boldsymbol{u}_{pq,\min})_i < k^{pr} \cdot (\boldsymbol{u}_p)_r < (\boldsymbol{u}_{pq,\max})_i$$

where $(\boldsymbol{u}_p)_r$ corresponds to $(\boldsymbol{u}_{pq})_i$ for some integer r.

b) If $(\boldsymbol{u}_{pq})_i$ is a control input belonging only to mode$_q$

$$(\boldsymbol{u}_{pq,\min})_i < k^{qr} \cdot (\boldsymbol{u}_q)_r < (\boldsymbol{u}_{pq,\max})_i$$

where $(\boldsymbol{u}_q)_r$ corresponds to $(\boldsymbol{u}_{pq})_i$ for some integer r.

c) If $(\boldsymbol{u}_{pq})_i$ is a control input belonging to mode$_p$ and mode$_q$

$$(\boldsymbol{u}_{pq,\min})_i < k^{pr} \cdot (\boldsymbol{u}_p)_r + k^{qs} \cdot (\boldsymbol{u}_q)_s < (\boldsymbol{u}_{pq,\max})_i$$

where $(\boldsymbol{u}_p)_r$ and $(\boldsymbol{u}_q)_s$ correspond to $(\boldsymbol{u}_{pq})_i$, for some integers r and s; where $(\boldsymbol{u}_{pq})_i$ is the ith element of $\boldsymbol{u}_{pq}$; $(\boldsymbol{u}_{pq,\min})_i$ and $(\boldsymbol{u}_{pq,\max})_i$ denote the minimum and maximum values of $(\boldsymbol{u}_{pq})_i$, respectively; and $(\boldsymbol{u}_p)_r$ and $(\boldsymbol{u}_q)_s$ denote the rth and sth elements of $\boldsymbol{u}_p$ and $\boldsymbol{u}_q$, respectively. Let $\boldsymbol{k}_{pq} = (k^{p1}, k^{p2}, \ldots, k^{pm_p}, k^{q1}, k^{q2}, \ldots, k^{qm_q})$.

The elements of $\boldsymbol{k}_{pq}$ are partitioned heuristically. The number of cells in the region of interest of $\boldsymbol{k}_{pq}$ is

$$\prod_{i=1}^{m_p+m_q} M_i$$

where M_i is the number of interval divisions along the ith element of $\boldsymbol{k}_{pq}$.

5) Determine the nonzero elements of $\boldsymbol{K}_p$ and $\boldsymbol{K}_q$ to transition from mode$_p$ to mode$_q$. The PPAA uses the region of interest and the partition information of $\boldsymbol{x}_{pq}$ and $\boldsymbol{k}_{pq}$ to produce a fuzzy controller that can be used to blend the outputs of the mode$_p$ and mode$_q$ controllers to obtain a mode$_p$-to-mode$_q$ transition. The inputs and outputs of the fuzzy controller are $\boldsymbol{x}_{pq}$ and $\boldsymbol{k}_{pq}$, respectively. The elements of $\boldsymbol{k}_{pq}$ are determined by the compositional rule of inference and the modified mean-of-maxima defuzzifier. The fuzzy linguistic rules for the fuzzy controller have the following form:

IF $(\boldsymbol{x}_{pq})_1$ is $L_{(\boldsymbol{x}_{pq})_1}$ and $\cdots$ and $(\boldsymbol{x}_{pq})_{n_{pq}}$ is $L_{(\boldsymbol{x}_{pq})_{n_{pq}}}$
THEN $(\boldsymbol{k}_{pq})_1$ is $L_{(\boldsymbol{k}_{pq})_1}$ and $\cdots$ and $(\boldsymbol{k}_{pq})_{m_p+m_q}$ is $L_{(\boldsymbol{k}_{pq})_{m_p+m_q}}$

where $(\boldsymbol{x}_{pq})_i$ and $(\boldsymbol{k}_{pq})_j$ are fuzzy representations for $(\boldsymbol{x}_{pq}(t))_i$ and $(\boldsymbol{k}_{pq}(t))_j$, the elements of $\boldsymbol{x}_{pq}(t)$ and $\boldsymbol{k}_{pq}(t)$, respectively; $L_{(\boldsymbol{x}_{pq})_i}$ and $L_{(\boldsymbol{k}_{pq})_j}$ are linguistic variables such as "positive large," "negative small."

Therefore, the mode$_p$-to-mode$_q$ controller will have the form

$$\boldsymbol{C}_{pq}(\boldsymbol{x}_{pq}, \boldsymbol{u}_p, \boldsymbol{u}_q) = \boldsymbol{K}_p(\boldsymbol{x}_{pq}) \cdot \boldsymbol{u}_p + \boldsymbol{K}_q(\boldsymbol{x}_{pq}) \cdot \boldsymbol{u}_q$$

where the nonzero elements of $\boldsymbol{K}_p$ and $\boldsymbol{K}_q$ are determined by a (n_{pq}-input, ($m_p + m_q$)-output) fuzzy controller.

Note that the mode-to-mode transition problem, as formulated, simplifies by assuming one nominal initial condition and reference trajectory. It is possible to extend the approach to the design of controllers that takes initial states in the neighborhood of the nominal initial condition to the specified final state. This can be accomplished by adapting the blending the gains such that the mode$_p$-to-mode$_q$ controller tracks the nominal reference trajectory in the least-squares sense.

B. Formulation of Fuzzy Logic Controller Robustness

Consider a nonlinear autonomous system that includes the dynamics of mode$_p$, mode$_q$, and their corresponding coupling dynamics,

$$\dot{\boldsymbol{x}} = \boldsymbol{f}(\boldsymbol{x}, \boldsymbol{u}, \boldsymbol{\alpha}), \qquad \boldsymbol{x}(t_0) = \boldsymbol{x}_0 \tag{1}$$

where $\boldsymbol{x}$ denotes the n_{pq}-dimensional state vector, $\boldsymbol{\alpha} = \boldsymbol{\alpha}_0 + \Delta\boldsymbol{\alpha}$ is an r-dimensional parameter vector, $\boldsymbol{f}$ is an n_{pq}-dimensional vector function, $\boldsymbol{u} = \boldsymbol{C}_{pq}(\boldsymbol{x}, \boldsymbol{\alpha}_0)$ is the m_{pq}-dimensional input vector generated by the mode$_p$-to-mode$_q$ fuzzy controller, $\boldsymbol{\alpha}_0$ is the nominal value of $\boldsymbol{\alpha}$, and $\Delta\boldsymbol{\alpha}$ is the vector of small perturbation about the nominal value.

Let $\boldsymbol{x}^*(t) = \boldsymbol{x}(t, \boldsymbol{\alpha}_0, \boldsymbol{x}_0^*)$ denote the nominal trajectory that satisfies

$$\dot{\boldsymbol{x}}^* = \boldsymbol{f}(\boldsymbol{x}^*, \boldsymbol{u}, \boldsymbol{\alpha}_0), \qquad \boldsymbol{x}^*(t_0) = \boldsymbol{x}_0^*$$

Let $\boldsymbol{x}(t) = \boldsymbol{x}(t, \boldsymbol{\alpha}, \boldsymbol{x}_0)$ denote the perturbed trajectory that satisfies

$$\dot{\boldsymbol{x}} = \boldsymbol{f}(\boldsymbol{x}, \boldsymbol{u}, \boldsymbol{\alpha}), \qquad \boldsymbol{x}(t_0) = \boldsymbol{x}_0$$

Define the error between the nominal and perturbed trajectory as

$$\begin{aligned} \boldsymbol{e}(t) &= \boldsymbol{e}(t, \boldsymbol{\alpha}, \boldsymbol{x}_0) \\ &= \boldsymbol{x}(t, \boldsymbol{\alpha}, \boldsymbol{x}_0) - \boldsymbol{x}\left(t, \boldsymbol{\alpha}_0, \boldsymbol{x}_0^*\right) \\ &= \boldsymbol{x}(t) - \boldsymbol{x}^*(t) \end{aligned} \tag{2}$$

Therefore the error dynamics can be represented as

$$\begin{aligned} &\dot{\boldsymbol{e}}(t) = \dot{\boldsymbol{x}}(t) - \dot{\boldsymbol{x}}^*(t) \\ &\Rightarrow \dot{\boldsymbol{e}} = f\left[\boldsymbol{e} + \boldsymbol{x}^*, \boldsymbol{C}_{pq}(\boldsymbol{x}, \boldsymbol{\alpha}_0), \boldsymbol{\alpha}, t\right] \\ &\quad - f\left[\boldsymbol{x}^*, \boldsymbol{C}_{pq}\left(\boldsymbol{x}^*, \boldsymbol{\alpha}_0\right), \boldsymbol{\alpha}_0, t\right] \\ &\Rightarrow \dot{\boldsymbol{e}} = \boldsymbol{g}(\boldsymbol{e}, t), \qquad \boldsymbol{g}(\boldsymbol{0}, t) = \boldsymbol{0} \end{aligned} \tag{3}$$

Because $\boldsymbol{x}^*(t)$ converges asymptotically from the equilibrium of mode$_p$ to the equilibrium of mode$_q$, then the stability of the nominal trajectory subjected to small perturbations of plant parameters and initial conditions will be examined. Investigating the stability of the nominal trajectory corresponds to the study of the stability of the trivial solution $\boldsymbol{y}(t) \equiv 0$ of the following equation:

$$\dot{\boldsymbol{y}} = \boldsymbol{g}(\boldsymbol{y}, t), \qquad \boldsymbol{g}(\boldsymbol{0}, t) = \boldsymbol{0} \tag{4}$$

The stability envelope of $\boldsymbol{x}^*(t)$, shown in Fig. 2, denotes the region about $\boldsymbol{x}^*(t)$ in which the perturbed trajectories must be constrained for the closed-loop system to be considered stable. In other words, the mode$_p$-to-mode$_q$ fuzzy controller possesses robust stability if the perturbed trajectories remain close to the nominal trajectory, as defined by the stability envelope when the system is subjected to small perturbations of plant parameters and initial conditions. The boundaries of the stability envelope satisfy the following relationship:

$$\boldsymbol{x}_{\max}(t) = \boldsymbol{x}^*(t) + \Delta x > \boldsymbol{x}^*(t) > \boldsymbol{x}^*(t) - \Delta\boldsymbol{x} = \boldsymbol{x}_{\min}(t) \tag{5}$$

where $\Delta\boldsymbol{x}$ is a positive vector. Therefore, the error between the nominal and perturbed trajectory satisfies the following condition:

$$|e_i(t)| \le (\Delta\boldsymbol{x})_i, \qquad \text{for} \qquad i = 1, \ldots, n_{pq} \tag{6}$$

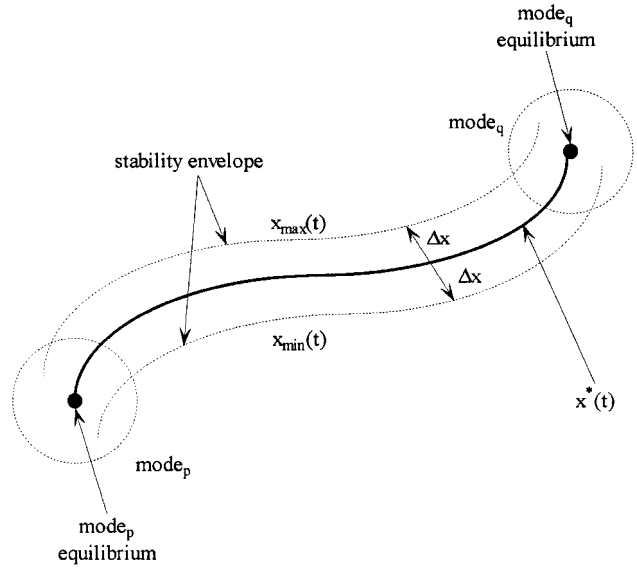

Fig. 2 Stability envelope of mode$_p$-to-mode$_q$ trajectory.

Definition 1. The trivial solution $\boldsymbol{y}(t) \equiv \boldsymbol{0}$ of Eq. (4) is called Lyapunov stable if for any $\varepsilon > 0$ there exists a $\delta(\varepsilon, t_0) > 0$ such that the inequality $|\boldsymbol{y}(t)| \le \varepsilon$ is satisfied for any $t \ge t_0$ whenever $|\boldsymbol{y}(t_0)| \le \delta(\varepsilon, t_0)$.

Definition 2. The trivial solution $\boldsymbol{y}(t) = 0$ of Eq. (4) is called uniformly stable with respect to t_0 if for any $\varepsilon > 0$ there exists a $\delta(\varepsilon) > 0$ independent of t_0 such that the inequality $|\boldsymbol{y}(t)| \le \varepsilon$ is satisfied for any $t \ge t_0$ whenever $|\boldsymbol{y}(t_0)| \le \delta(\varepsilon)$.

Definition 3. A continuous function ω: $R^+ \to R^+$ is said to be of class K (or to belong to class K), if 1) $\omega(0) = 0$, 2) $\omega(p) > 0$, and $\forall p > 0$, and 3) ω is nondecreasing.

Theorem 1. Assume that, in a neighborhood of $\boldsymbol{y}(t) \equiv \boldsymbol{0}$ in Eq. (4), there exists a scalar function $V(\boldsymbol{y}, t)$ with continuous first-order derivatives and a class-K function w_1 such that $\forall \boldsymbol{y} \ne 0$: 1) $V(\boldsymbol{y}, t) \ge w_1(\|\boldsymbol{y}\|) > 0$, and 2) $\dot{V}(\boldsymbol{y}, t) \le 0$, then $\boldsymbol{y}(t) = \boldsymbol{0}$ is Lyapunov stable. If, furthermore, there is a scalar class-K function w_2 such that $V(\boldsymbol{y}, t) \le w_2(\|\boldsymbol{y}\|)$, then $\boldsymbol{y}(t) = \boldsymbol{0}$ is uniformly stable.

Proof. The proof of this theorem can be found in Ref. 8.

Definition 4. Define a unit parameter perturbation as

$$\Delta\alpha_i/\alpha_i = k_{ii} \in R, \qquad i = 1, \ldots, r \tag{7}$$

Definition 5. The fuzzy sensitivity of the real output function, $e(\boldsymbol{x}, \boldsymbol{\alpha}, t)$, with respect to the real parameters α_i, $i = 1, \ldots, r$, is expressed by[1]

$$S_\alpha^e = \frac{1 - \mu_{\Delta e}}{1 - w_1\mu_{\Delta\alpha_1} - w_2\mu_{\Delta\alpha_2} - \cdots - w_r\mu_{\Delta\alpha_r}}, \qquad \sum_{i=1}^{r} w_i = 1$$

$$w_i \in [0, 1] \tag{8}$$

where μ are membership functions of the deviations and w_i are weights that are heuristically chosen to signify the importance of a parameter.

Definition 6. The single parameter fuzzy sensitivity expression with parameter α_i giving rise to a change in e_j is written as

$$S_{\alpha_i}^{e_j} = \frac{1 - \mu_{\Delta e_j}}{1 - \mu_{\Delta\alpha_i}} \tag{9}$$

The sensitivity $S_{\alpha_i}^{e_j}$ is calculated by fixing the other parameters $\alpha_{j, j \ne i}$ to their nominal values. In the following development of robust stability, the single parameter expression will be used for fuzzy sensitivity.

C. Main Robust Stability Results

Theorem 2. Let the fuzzy controller $\boldsymbol{C}_{pq}(\boldsymbol{x}, \boldsymbol{\alpha}_0)$ transition from mode$_p$ to mode$_q$ stably for the system given in Eq. (1) having

nominal parameters. The fuzzy controller $\boldsymbol{C}_{pq}(\boldsymbol{x}, \boldsymbol{\alpha}_0)$ is robust with respect to parametric uncertainty if the following condition is satisfied:

$$\boldsymbol{P} = \begin{bmatrix} \sum_{j=1}^{r} S_{\alpha_j}^{e_1} k_{jj} & 0 & \cdots & 0 \\ 0 & \sum_{j=1}^{r} S_{\alpha_j}^{e_2} k_{jj} & \cdots & 0 \\ \vdots & \vdots & \ddots & \vdots \\ 0 & 0 & \cdots & \sum_{j=1}^{r} S_{\alpha_j}^{e_{npq}} k_{jj} \end{bmatrix} \leq 0 \qquad \forall t \geq t_0 \quad (10)$$

Proof. Because we want the perturbed trajectories to remain close to the nominal trajectory when subjected to parameter and initial condition variations, then the performance measure should incorporate information about the error between the trajectories. Let us define the performance measure as a lower-bounded function given by

$$V(\boldsymbol{e}, t) = \tfrac{1}{2}\boldsymbol{e}^T\boldsymbol{e} \quad (11)$$

where $\boldsymbol{e}(t)$ is defined in Eq. (2).

From a stability standpoint, $\boldsymbol{C}_{pq}(\boldsymbol{x}, \boldsymbol{\alpha}_0)$ is required to ensure that $\forall \boldsymbol{e} \neq \boldsymbol{0}$:

$$V(\boldsymbol{e}, t) \geq w_1(\|\boldsymbol{e}\|) > 0, \qquad \dot{V}(\boldsymbol{e}, t) \leq 0$$

where $w_1(\|\boldsymbol{e}\|)$ is a class-K function. Let $w_1(\|\boldsymbol{e}\|) = \frac{1}{4}\{\|\boldsymbol{e}\|\}^2 = \frac{1}{4}\boldsymbol{e}^T\boldsymbol{e}$, which is a class-K function. Because $w_1(\|\boldsymbol{e}\|)$ is a class-K function and $V(\boldsymbol{e}, t) \geq w_1(\|\boldsymbol{e}\|) > 0$ ($\forall \boldsymbol{e} \neq \boldsymbol{0}$), then the nominal trajectory is stable if the following condition is met:

$$\dot{V}(\boldsymbol{e}, t) \leq 0, \qquad \forall t \geq t_0, \qquad \text{or} \qquad \mathrm{d}V(\boldsymbol{e}, t) \leq 0, \qquad \forall t \geq t_0$$

Therefore,

$$\mathrm{d}V(\boldsymbol{e}, t) = \mathrm{d}V(\boldsymbol{e}) = \boldsymbol{e}^T\mathrm{d}\boldsymbol{e}, \qquad \mathrm{d}\boldsymbol{e} = \begin{bmatrix} \frac{\partial e_1}{\partial \alpha_1} & \cdots & \frac{\partial e_1}{\partial \alpha_r} \\ \vdots & \ddots & \vdots \\ \frac{\partial e_{npq}}{\partial \alpha_1} & \cdots & \frac{\partial e_{npq}}{\partial \alpha_r} \end{bmatrix} \mathrm{d}\boldsymbol{\alpha} \quad (12)$$

Consider the most general notion of sensitivity from a control-theoretic viewpoint. The sensitivity of an observed variable ζ, which is a function of the parameter α, is defined as the percentage change in the quantity ζ divided by the percentage change in the parameter α that caused the change in ζ. The most commonly used expression is

$$S_{\alpha}^{\zeta} = \frac{\partial \zeta / \zeta}{\partial \alpha / \alpha} \quad (13)$$

Therefore, the sensitivity of e_j with respect to the parameter α_i is

$$S_{\alpha_i}^{e_j} = \frac{\partial e_j / e_j}{\partial \alpha_i / \alpha_i} = \frac{\partial e_j}{\partial \alpha_i}\frac{\alpha_i}{e_j} \quad (14)$$

The sensitivity expression in Eq. (14), therefore, will be approximated by the single parameter fuzzy sensitivity expression given in Eq. (9).

Comparing Eqs. (9) and (14) gives

$$S_{\alpha_i}^{e_j} = \frac{\partial e_j / e_j}{\partial \alpha_i / \alpha_i} \approx \frac{1 - \mu_{\Delta e_j}}{1 - \mu_{\Delta \alpha_i}} \quad (15)$$

Now, the partial derivatives in Eq. (12) can be approximated by

$$\frac{\partial e_j}{\partial \alpha_i} \approx \frac{1 - \mu_{\Delta e_j}}{1 - \mu_{\Delta \alpha_i}}\frac{e_j}{\alpha_i} \quad (16)$$

Using Eqs. (12–16), the expression for $\mathrm{d}V(\boldsymbol{e}, t)$ becomes

$$\mathrm{d}V(\boldsymbol{e}, t) = \boldsymbol{e}^T \begin{bmatrix} (e_1/\alpha_1) S_{\alpha_1}^{e_1} & \cdots & (e_1/\alpha_r) S_{\alpha_r}^{e_1} \\ \vdots & \ddots & \vdots \\ \left(e_{n_{pq}}/\alpha_1\right) S_{\alpha_1}^{e_{npq}} & \cdots & \left(e_{n_{pq}}/\alpha_r\right) S_{\alpha_r}^{e_{npq}} \end{bmatrix} \mathrm{d}\boldsymbol{\alpha} \quad (17)$$

$$\mathrm{d}V(\boldsymbol{e}, t) = \boldsymbol{e}^T \begin{bmatrix} e_1 k_{11} S_{\alpha_1}^{e_1} + \cdots + e_1 k_{rr} S_{\alpha_r}^{e_1} \\ \vdots \\ e_{n_{pq}} k_{11} S_{\alpha_1}^{e_{npq}} + \cdots + e_{n_{pq}} k_{rr} S_{\alpha_r}^{e_{npq}} \end{bmatrix} \quad (18)$$

$$\mathrm{d}V(\boldsymbol{e}, t) = \boldsymbol{e}^T \begin{bmatrix} \sum_{j=1}^{r} S_{\alpha_j}^{e_1} k_{jj} & 0 & \cdots & 0 \\ 0 & \sum_{j=1}^{r} S_{\alpha_j}^{e_2} k_{jj} & \cdots & 0 \\ \vdots & \vdots & \ddots & \vdots \\ 0 & 0 & \cdots & \sum_{j=1}^{r} S_{\alpha_j}^{e_{npq}} k_{jj} \end{bmatrix} \boldsymbol{e}$$

$$= \boldsymbol{e}^T \boldsymbol{P} \boldsymbol{e} \quad (19)$$

Then

$$\boldsymbol{P} \leq 0 \Rightarrow \mathrm{d}V(\boldsymbol{e}, t) \leq 0$$

Theorem 3. Let the fuzzy controller $\boldsymbol{C}_{pq}(\boldsymbol{x}, \boldsymbol{\alpha}_0)$ transition from mode$_p$ to mode$_q$ stably for the system given in Eq. (1) having nominal initial condition. The fuzzy controller $\boldsymbol{C}_{pq}(\boldsymbol{x}, \boldsymbol{\alpha}_0)$ is robust with respect to perturbed initial conditions if the following condition is satisfied:

$$\boldsymbol{P} = \begin{bmatrix} \sum_{j=1}^{n_{pq}} S_{(x_0)_j}^{e_1} \bar{k}_{jj} & 0 & \cdots & 0 \\ 0 & \sum_{j=1}^{n_{pq}} S_{(x_0)_j}^{e_2} \bar{k}_{jj} & \cdots & 0 \\ \vdots & \vdots & \ddots & \vdots \\ 0 & 0 & \cdots & \sum_{j=1}^{n_{pq}} S_{(x_0)_j}^{e_{npq}} \bar{k}_{jj} \end{bmatrix} \leq 0 \qquad \forall t \geq t_0 \quad (20)$$

where $\bar{k}_{jj} = (\Delta \boldsymbol{x}_0)_j / (\boldsymbol{x}_0)_j$ and $\Delta \boldsymbol{x}_0 = \boldsymbol{x}_0 - \boldsymbol{x}_0^*$.

Proof. Use the proof of Theorem 2, although substituting $\boldsymbol{x}_0$ for $\boldsymbol{\alpha}$, $\Delta \boldsymbol{x}_0$ for $\boldsymbol{\Delta \alpha}$, and $\bar{k}_{jj}$ for k_{jj}.

D. Determine Worst-Case dV

The objective is to find $\mathrm{d}V(\boldsymbol{e}, t)$ that corresponds to the worst-case trajectory errors. The worst-case trajectory errors is determined by maximizing a function of these errors in the space parameter perturbations. The worst-case $\mathrm{d}V(\boldsymbol{e}, t)$ can be determined several ways:

1) Find $\mathrm{d}V_{\text{worst case}}$ such that $h(\boldsymbol{e}) = \boldsymbol{e}^T(t_f)\boldsymbol{e}(t_f)$ is maximized, i.e., find $\mathrm{d}V_{\text{worst case}}$ such that the steady-state errors from the nominal trajectory are maximized.

2) Find $\mathrm{d}V_{\text{worst case}}$ such that

$$h(\boldsymbol{e}) = \int_{t_0}^{t_f} \boldsymbol{e}^T(t)\boldsymbol{e}(t)\,\mathrm{d}t$$

is maximized, i.e., find $\mathrm{d}V_{\text{worst case}}$ such that the trajectory error in the time interval $[t_0, t_f]$ is a maximum.

3) Find $dV_{\text{worst case}}$ such that $h(\boldsymbol{e}) = \sup_t\{\boldsymbol{e}^T(t)\boldsymbol{e}(t)\}$ is maximized, i.e., find $dV_{\text{worst case}}$ such that the magnitude of trajectory error is maximized.

Even if $dV_{\text{worst case}}$ is found such that $h(\boldsymbol{e})$ is maximized, this does not tell us how to select the worst-case sensitivities. Without this maximization, though, it would be difficult to determine the worst-case performance in terms of trajectory errors. Key robustness questions are: 1) How large can k_{jj} be?, 2) How large can $S^{e_i}_{\alpha_j}$ be?, and 3) How large can $S^{e_i}_{\alpha_j} k_{jj}$ be before the system is destabilized?; i.e., before

$$\sum_{j=1}^{r} S^{e_i}_{\alpha_j} k_{jj} \le 0, \qquad \text{for} \qquad i = 1, \ldots, n_{pq}$$

Note that the preceding discussion is also applicable to the case of perturbed initial conditions.

E. Measure of Robustness

The measure of the size of the matrix $\boldsymbol{P}$ in Eqs. (10) or (20) is given by[1,2]

$$\|\boldsymbol{P}\|_\infty = \sup_t \bar{\sigma}(\boldsymbol{P}, t) \tag{21}$$

where $\bar{\sigma}(\boldsymbol{P}, t)$ denotes the maximum singular value of the time-varying matrix $\boldsymbol{P}$.

Because the sensitivities of the trajectory errors defined in Eq. (2) are incorporated into the matrix $\boldsymbol{P}$, then the supremum of the maximum singular value of $\boldsymbol{P}$ will be used as a measure of robustness. The fuzzy robustness measure (FRM) is given by

$$\text{FRM} = \|\boldsymbol{P}\|_\infty \tag{22}$$

The feasible universe of discourse for the fuzzy robustness measure is considered to be $[\text{FRM}_{\min}, \text{FRM}_{\max}]$. The computed value of FRM will have membership in this interval that can be described linguistically in terms of fuzzy sets. The smaller the value of FRM, the more robust is the closed-loop system.

F. Robust Analysis

Definition 7. Worst-case sensitivity is such that a "small" parameter perturbation leads to the largest change in the trajectory error. In other words, $(1 - \mu_{\Delta\alpha_i}) \rightarrow 0$ such that $(1 - \mu_{\Delta e_j}) \rightarrow 1$.

Definition 8. Ideal-case sensitivity is such that the trajectory error is unaffected by parameter perturbations. In other words, $(1 - \mu_{\Delta e_j})/(1 - \mu_{\Delta\alpha_i}) \approx 0$.

The robust analysis is performed to identify the least robust perturbation over a space of possible parameter variations. The analysis procedure is summarized as follows.

1) Determine the nominal trajectory $\boldsymbol{x}^*(t)$ by simulating the closed-loop system using the nominal parameter values.

2) Specify the membership functions $\mu_{\Delta\alpha_i}$ and $\mu_{\Delta e_j}$ of the deviations for $\Delta\alpha_i$ and Δe_j. Figure 3 shows the fuzzy sets for small parameter perturbations and trajectory deviations from the nominal trajectory.

3) Calculate $S^{e_j}_{\alpha_i}$ in the following way:

a) Determine the perturbed trajectory $\boldsymbol{x}(t)$ by simulating the closed-loop system using the parameter vector $\boldsymbol{\alpha} = \boldsymbol{\alpha}_0 + \Delta\boldsymbol{\alpha}$, where $\Delta\alpha_i \neq 0$ and $\Delta\alpha_{j,j\neq i} = 0$.

b) Given $\mu_{\Delta\alpha_i}$ and $\mu_{\Delta e_j}$, calculate $S^{e_j}_{\alpha_i}$ using Eq. (2) and Definition 6.

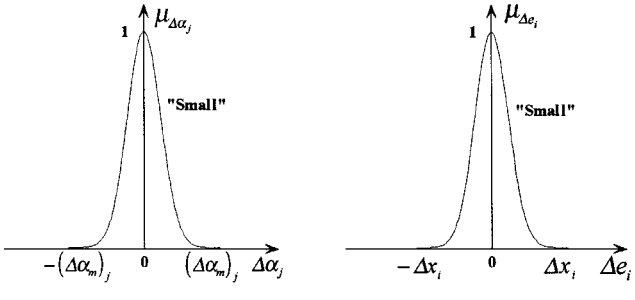

Fig. 3 Fuzzy set for small perturbations and trajectory deviations.

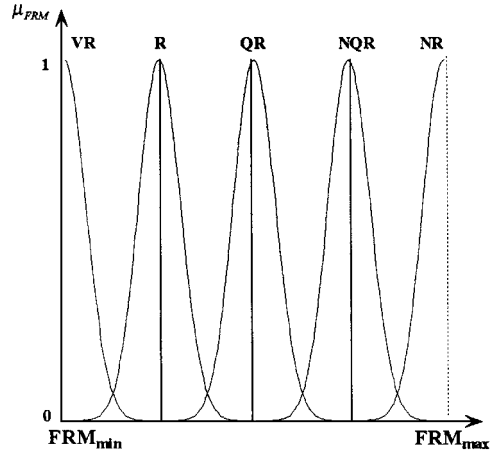

Fig. 4 Fuzzy robust measure. VR = very robust; R = robust; QR = quite robust; NR = not robust; NQR = not quite robust.

4) Calculate $\text{FRM}_{\min}$, $\text{FRM}_{\max}$, and $h_{\max}$. The $\text{FRM}_{\min}$ and $\text{FRM}_{\max}$ correspond to calculating FRM assuming worst-case and ideal-case sensitivity, respectively. The value $h_{\max}$ is chosen by the designer and designates the value of $h(\boldsymbol{e})$ beyond which trajectory errors are not acceptable. Figure 4 shows the fuzzy sets for linguistic values of "very robust," "robust," "quite robust," "not quite robust," and "not robust."

5) Determine $\text{FRM}^*_{\max}$ and $dV_{\text{worst case}}$. The $\text{FRM}^*_{\max}$ is the maximum value of FRM determined over the space of parameter variations. The performance index $dV_{\text{worst case}}$ is selected such that $h(\boldsymbol{e})$ is maximized over the space of parameter variations. The $\text{FRM}^*_{\max}$ and $h^*_{\max}$ are the maximum value of FRM and $h(\boldsymbol{e})$ determined over the space of parameter variations. A linguistic value is assigned to $\text{FRM}^*_{\max}$ from Fig. 4, while the $h^*_{\max}$ is compared with $h_{\max}$. Note that FRM and $h(\boldsymbol{e})$ are calculated using $\boldsymbol{e}(t) = \boldsymbol{x}(t) - \boldsymbol{x}^*(t)$, where $\boldsymbol{x}(t)$ is determined by simulating the closed-loop system using the parameter vector $\boldsymbol{\alpha} = \boldsymbol{\alpha}_0 + \Delta\boldsymbol{\alpha}$, $\Delta\alpha_i \neq 0$, for $i = 1, \ldots, r$.

6) Determine the least-robust perturbation by maximizing the following performance criteria:

$$\lambda_1 \cdot h(\boldsymbol{e}) + \lambda_2 \cdot \text{FRM}, \qquad \lambda_i \in [0, 1], \quad \lambda_1 + \lambda_2 = 1$$

where the weights λ_i are chosen heuristically and the function $h(\boldsymbol{e})$ is selected to be either

$$\boldsymbol{e}^T(t_f)\boldsymbol{e}(t_f), \qquad \int_{t_0}^{t_f} \boldsymbol{e}^T(t)\boldsymbol{e}(t)\,dt \quad \text{or} \quad \sup_t\{\boldsymbol{e}^T(t)\boldsymbol{e}(t)\}$$

The preceding robust analysis procedure is also applicable to the case of perturbed initial conditions.

III. Example: Hover to FF Fuzzy Controller

A. Parametric Model of Helicopter's Forward Dynamics

The proposed approach is used to analyze the robustness of the hover to FF transition controller for the following model representing the longitudinal channel dynamics of a small-scale helicopter constrained to have no vertical motion; only longitudinal and pitch rotation motions are allowed:

$$X = X_{\text{hov}} \cdot \mu_{\text{hov}} + X_{\text{FF}} \cdot \mu_{\text{FF}}, \qquad M = M_{\text{hov}} \cdot \mu_{\text{hov}} + M_{\text{FF}} \cdot \mu_{\text{FF}}$$

$$\ddot{x} = \frac{X}{m \cdot \cos(\theta)} - g \cdot \tan(\theta), \qquad \ddot{\theta} = \frac{M}{I_y}$$

$$X_{\text{hov}} = X_{\text{trim,hov}} + X_{\dot{x},\text{hov}}(\dot{x} - \dot{x}_{\text{trim,hov}}) + X_{\dot{\theta},\text{hov}}(\dot{\theta} - \dot{\theta}_{\text{trim,hov}}) + X_{\delta_e,\text{hov}}(\delta_e - \delta_{e,\text{trim,hov}})$$

$$X_{\text{FF}} = X_{\text{trim,FF}} + X_{\dot{x},\text{FF}}(\dot{x} - \dot{x}_{\text{trim,FF}}) + X_{\dot{\theta},\text{FF}}(\dot{\theta} - \dot{\theta}_{\text{trim,FF}}) + X_{\delta_e,\text{FF}}(\delta_e - \delta_{e,\text{trim,FF}})$$

$$M_{\text{hov}} = M_{\text{trim,hov}} + M_{\dot{x},\text{hov}}(\dot{x} - \dot{x}_{\text{trim,hov}})$$

Table 1 Aerodynamic parameters and the corresponding trim values

Parameter	Value	Description
$X_{\dot{x},\text{hov}}$	−0.0400	Partial derivative of X with respect to $\dot{x}$ at hover
$X_{\dot{\theta},\text{hov}}$	1.1675	Partial derivative of X with respect to $\dot{\theta}$ at hover
$X_{\delta_e,\text{hov}}$	21.2482	Partial derivative of X with respect to δ_e at hover
$X_{\text{trim,hov}}$	−0.1011	Trim value of aerodynamic force X at hover
$X_{\dot{x},\text{FF}}$	−0.0019	Partial derivative of X with respect to $\dot{x}$ at FF
$X_{\dot{\theta},\text{FF}}$	1.2018	Partial derivative of X with respect to $\dot{\theta}$ at FF
$X_{\delta_e,\text{FF}}$	26.9988	Partial derivative of X with respect to δ_e at FF
$X_{\text{trim,FF}}$	−0.5411	Trim value of aerodynamic force X at FF
$M_{\dot{x},\text{hov}}$	0.0000	Partial derivative of M with respect to $\dot{x}$ at hover
$M_{\dot{\theta},\text{hov}}$	−1.8769	Partial derivative of M with respect to $\dot{\theta}$ at hover
$M_{\delta_e,\text{hov}}$	−43.4060	Partial derivative of M with respect to δ_e at hover
$M_{\text{trim,hov}}$	0.0000	Trim value of aerodynamic moment M at hover
$M_{\dot{x},\text{FF}}$	0.0000	Partial derivative of M with respect to $\dot{x}$ at FF
$M_{\dot{\theta},\text{FF}}$	−1.6336	Partial derivative of M with respect to $\dot{\theta}$ at FF
$M_{\delta_e,\text{FF}}$	−37.4916	Partial derivative of M with respect to δ_e at FF
$M_{\text{trim,FF}}$	0.0000	Trim value of aerodynamic moment M at FF
$\dot{x}_{\text{trim,hov}}$	0.0000	Trim value of forward velocity $\dot{x}$ at hover
$\dot{\theta}_{\text{trim,hov}}$	0.0000	Trim value of pitch angle velocity $\dot{\theta}$ at hover
$\delta_{e,\text{trim,hov}}$	−0.0021	Trim value of longitudinal input δ_e at hover
$\dot{x}_{\text{trim,FF}}$	17.0000	Trim value of forward velocity $\dot{x}$ at FF
$\dot{\theta}_{\text{trim,FF}}$	0.0000	Trim value of pitch angle velocity $\dot{\theta}$ at FF
$\delta_{e,\text{trim,FF}}$	−0.0421	Trim value of longitudinal input δ_e at FF
$\theta_{\text{trim,hov}}$	−0.0037	Trim value of pitch angle θ at hover
$\theta_{\text{trim,FF}}$	−0.0198	Trim value of pitch angle θ at FF
m	0.8488	Mass of the helicopter
I_Y	0.7656	Moment of inertia along y axis

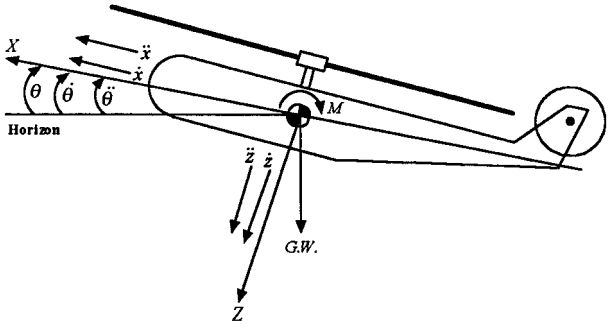

Fig. 5 Side view of helicopter's axis system.

$$+ M_{\dot{\theta},\text{hov}}(\dot{\theta} - \dot{\theta}_{\text{trim,hov}}) + M_{\delta_e,\text{hov}}(\delta_e - \delta_{e,\text{trim,hov}})$$

$$M_{\text{FF}} = M_{\text{trim,FF}} + M_{\dot{x},\text{FF}}(\dot{x} - \dot{x}_{\text{trim,FF}}) + M_{\dot{\theta},\text{FF}}(\dot{\theta} - \dot{\theta}_{\text{trim,FF}})$$

$$+ M_{\delta_e,\text{FF}}(\delta_e - \delta_{e,\text{trim,FF}})$$

$$\mu_{\text{hov}} = \begin{cases} 1, & \text{if} \quad |\dot{x}| < 3 \\ 0, & \text{if} \quad |\dot{x} - 17| < 3 \\ -\dfrac{\dot{x} - 14}{11}, & \text{if} \quad 3 \le \dot{x} \le 14 \end{cases}$$

$$\mu_{\text{FF}} = \begin{cases} 0, & \text{if} \quad |\dot{x}| < 3 \\ 1, & \text{if} \quad |\dot{x} - 17| < 3 \\ \dfrac{\dot{x} - 3}{11}, & \text{if} \quad 3 \le \dot{x} \le 14 \end{cases}$$

where $\ddot{x}$, $\ddot{\theta}$, and δ_e represent the forward acceleration (ft/s^2), pitch angle acceleration (rad/s^2), and longitudinal cyclic input (rad), respectively. The aerodynamic force along the x axis is represented by X, and M represents the pitching moment about the y axis. Figure 5 shows the axis system of the helicopter with respect to the side view. The aerodynamic parameters and corresponding trim values for the hover and FF are given in Table 1. These constant values were calculated by a trim analysis program using physical parameters from a Xcell 300 helicopter in hover and FF. The state vector of the helicopter model is $[x_1 \;\; x_2 \;\; x_3 \;\; x_4]^T = [\dot{x} \;\; \ddot{x} \;\; \boldsymbol{\theta} \;\; \dot{\boldsymbol{\theta}}]^T$. It is assumed that the output vector of the model is the same as the state vector. To perform a parametric analysis, the model can be transformed into the following form:

$$\ddot{x} = \frac{X}{\tilde{\alpha}_3 c_{31} \cdot \cos(\theta)} - g \cdot \tan(\theta), \qquad \ddot{\theta} = \frac{M}{\tilde{\alpha}_6 c_{61}}$$

$$X = X_{\text{hov}} \cdot \mu_{\text{hov}} + X_{\text{FF}} \cdot \mu_{\text{FF}}, \qquad M = M_{\text{hov}} \cdot \mu_{\text{hov}} + M_{\text{FF}} \cdot \mu_{\text{FF}}$$

$$X_{\text{hov}} = \tilde{\alpha}_1(c_{11} + c_{12}\Delta\dot{x}_{\text{hov}} + c_{13}\Delta\dot{\theta}_{\text{hov}} + c_{14}\Delta\delta_{e,\text{hov}})$$

$$X_{\text{FF}} = \tilde{\alpha}_2(c_{21} + c_{22}\Delta\dot{x}_{\text{FF}} + c_{23}\Delta\dot{\theta}_{\text{FF}} + c_{24}\Delta\delta_{e,\text{FF}})$$

$$M_{\text{hov}} = \tilde{\alpha}_4(c_{41} + c_{42}\Delta\dot{x}_{\text{hov}} + c_{43}\Delta\dot{\theta}_{\text{hov}} + c_{44}\Delta\delta_{e,\text{hov}})$$

$$M_{\text{FF}} = \tilde{\alpha}_5(c_{51} + c_{52}\Delta\dot{x}_{\text{FF}} + c_{53}\Delta\dot{\theta}_{\text{FF}} + c_{54}\Delta\delta_{e,\text{FF}})$$

where the parameters have the following values: $\tilde{\alpha}_1 = 10.00$ is the nominal gain for the hover aerodynamic force; $\tilde{\alpha}_2 = 10.00$ is the nominal gain for the FF aerodynamic force; $\tilde{\alpha}_3 = 10.00$ is the nominal gain for the helicopter's mass; $\tilde{\alpha}_4 = 10.00$ is the nominal gain for the hover aerodynamic moment; $\tilde{\alpha}_5 = 10.00$ is the nominal gain for the FF aerodynamic moment; and $\tilde{\alpha}_6 = 10.00$ is the nominal gain for the moment of inertia along the y axis. The constant values are

$$c_{11} = -0.0101, \quad c_{12} = -0.0040, \quad c_{13} = 0.1168$$
$$c_{14} = 2.1248, \quad c_{21} = -0.0541, \quad c_{22} = -0.0002$$
$$c_{23} = 0.1202, \quad c_{24} = 2.6999, \quad c_{31} = 0.0849$$
$$c_{41} = 0.0000, \quad c_{42} = 0.0000, \quad c_{43} = -0.1877$$
$$c_{44} = -4.3406, \quad c_{51} = 0.0000, \quad c_{52} = 0.0000$$
$$c_{53} = -0.1634, \quad c_{54} = -3.7492, \quad c_{61} = 0.0766$$

B. Hover to FF Mode Controller

The following control law was used for the hover to FF controller:

$$\delta_e = \delta_{e,\text{hov}}(\dot{x}, \theta, \dot{\theta}) \cdot K_{\text{hov}}(\dot{x}, \ddot{x}, \theta, \dot{\theta})$$

$$+ \delta_{e,\text{FF}}(\dot{x}, \ddot{x}, \theta, \dot{\theta}) \cdot K_{\text{FF}}(\dot{x}, \ddot{x}, \theta, \dot{\theta})$$

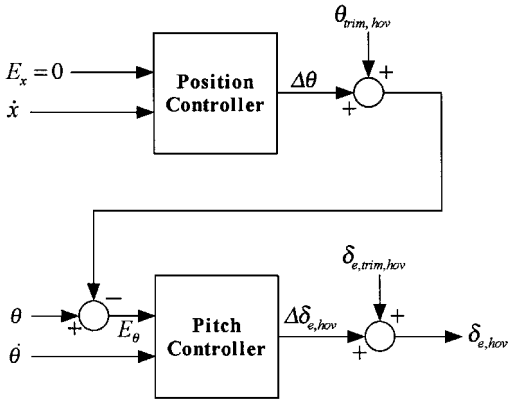

E_x

$\dot{x}$ \ $\Delta\theta$	N	Z	P
N	NM	NM	PS
Z	NM	Z	PM
P	NS	PM	PM

Position Controller Rulebase

E_θ

$\dot{\theta}$ \ $\Delta\delta_{e,hov}$	N	Z	P
N	NM	NM	PS
Z	NM	Z	PM
P	NS	PM	PM

Pitch Controller Rulebase

Fig. 6 Structure of hover mode controller.

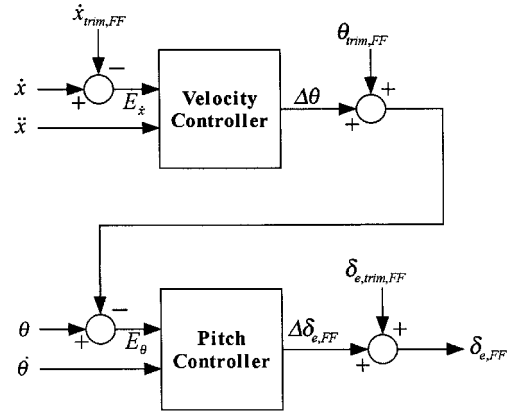

$E_{\dot{x}}$

$\ddot{x}$ \ $\Delta\theta$	N	Z	P
N	Z	Z	PM
Z	NS	Z	PS
P	NM	Z	Z

Velocity Controller Rulebase

E_θ

$\dot{\theta}$ \ $\Delta\delta_{e,FF}$	N	Z	P
N	NM	NM	PS
Z	NM	Z	PM
P	NS	PM	PM

Pitch Controller Rulebase

Fig. 7 Structure of FF mode controller.

where $\delta_{e,\mathrm{hov}}(\cdot)$ and $\delta_{e,\mathrm{FF}}(\cdot)$ are fuzzy regulators for the hover and FF modes. Note that $\delta_{e,\mathrm{hov}}(\cdot)$, $\delta_{e,\mathrm{FF}}(\cdot)$, and δ_e are scalar. Figures 6 and 7 show the structure of the hover and FF controllers. The hover and FF controllers regulate about the operating points

$$[\dot{x} \quad \ddot{x} \quad \theta \quad \dot{\theta}]^T = [0.0000 \quad 0.0000 \quad -0.0037 \quad 0.0000]^T$$

$$[\dot{x} \quad \ddot{x} \quad \theta \quad \dot{\theta}]^T = [17.0000 \quad 0.0000 \quad -0.0198 \quad 0.0000]^T$$

respectively. The scalar gains $K_{\mathrm{hov}}(\dot{x}, \ddot{x}, \theta, \dot{\theta})$ and $K_{\mathrm{FF}}(\dot{x}, \ddot{x}, \theta, \dot{\theta})$ are determined via the PPAA such that closed-loop system transitions from

$$[0.0000 \quad 0.0000 \quad -0.0037 \quad 0.0000]^T$$

to

$$[17.0000 \quad 0.0000 \quad -0.0198 \quad 0.0000]^T$$

in minimum time with the following constraints:

$$-0.3148 \le \dot{x} \le 17.6296, \qquad -0.5000 \le \ddot{x} \le 2.5000$$

$$-0.1164 \le \theta \le 0.0124, \qquad -0.2400 \le \dot{\theta} \le 0.2400$$

$$-0.0625 \le K_{\mathrm{hov}} \le 1.0625, \qquad -0.0625 \le K_{\mathrm{FF}} \le 1.0625$$

C. Robust Analysis: Simulations

The robust stability of the mode$_{\mathrm{hover}}$-to-mode$_{\mathrm{FF}}$ fuzzy controller is studied when $\tilde{\alpha}_3$ and $\tilde{\alpha}_6$ are perturbed. Because we want $dV \le 0$, we need to perform a robust analysis where $\Delta\tilde{\alpha}_3$, $\Delta\tilde{\alpha}_6 \le 0$. Let $\boldsymbol{\alpha} = [\alpha_1 \ \alpha_2]^T$, where α_1 and α_2 denote the parameters $\tilde{\alpha}_3$ and $\tilde{\alpha}_6$, respectively.

Figures 8 and 9 show $\dot{x}$, $\ddot{x}$, θ, and $\dot{\theta}$ trajectories with respect to nominal parameter values. The robust analysis will be performed such that the perturbed trajectories are within the stability band represented by the following equation:

$$|e_j(t)| \le \Delta x_j, \qquad \text{for} \qquad j = 1, \ldots, 4$$

where

$$\Delta \boldsymbol{x} = [\Delta x_1 \quad \Delta x_2 \quad \Delta x_3 \quad \Delta x_4]^T = [0.50 \quad 0.90 \quad 0.03 \quad 0.15]^T$$

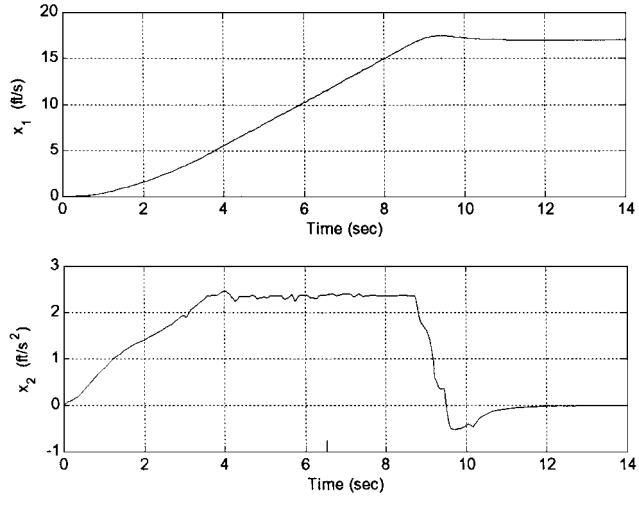

Fig. 8 Plots of $\dot{x}$ and $\ddot{x}$ nominal trajectories.

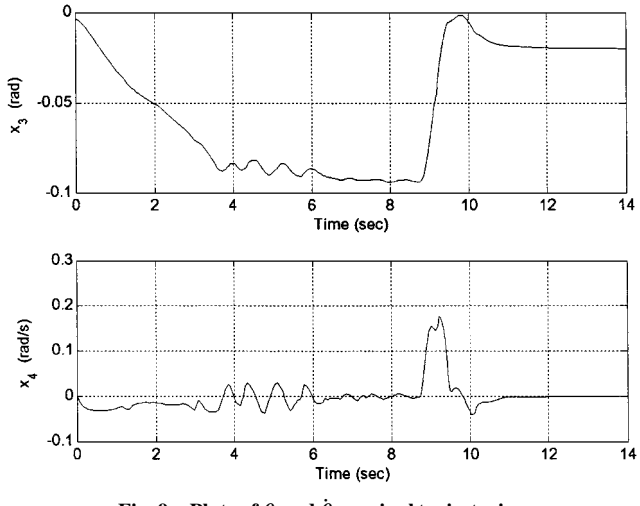

Fig. 9 Plots of θ and $\dot{\theta}$ nominal trajectories.

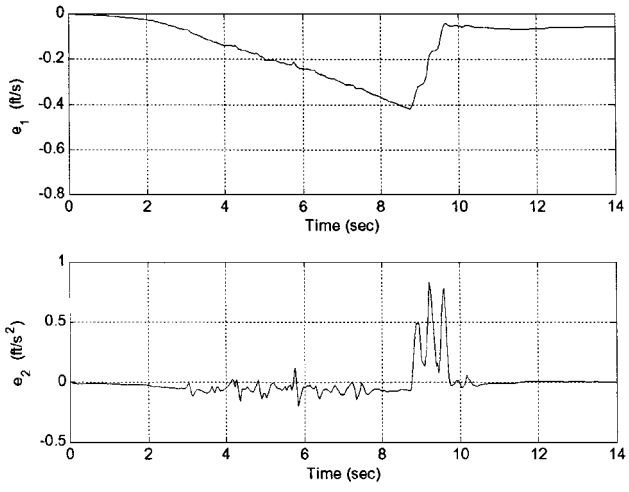

Fig. 10 Plots of $\dot{x}$ and $\ddot{x}$ trajectory errors for the least-robust operation.

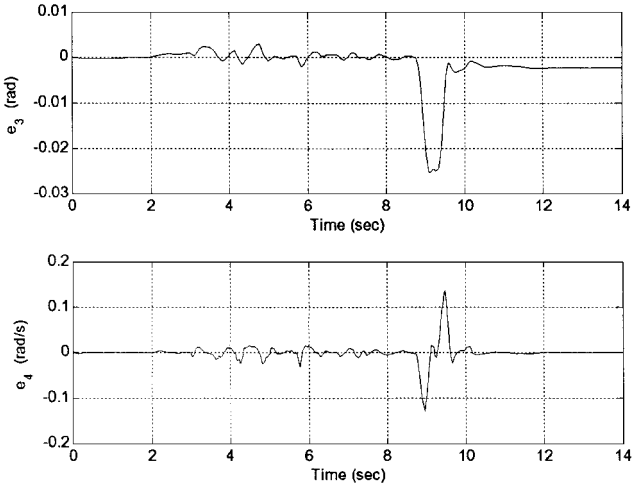

Fig. 11 Plots of θ and $\dot{\theta}$ trajectory errors for the least-robust operation.

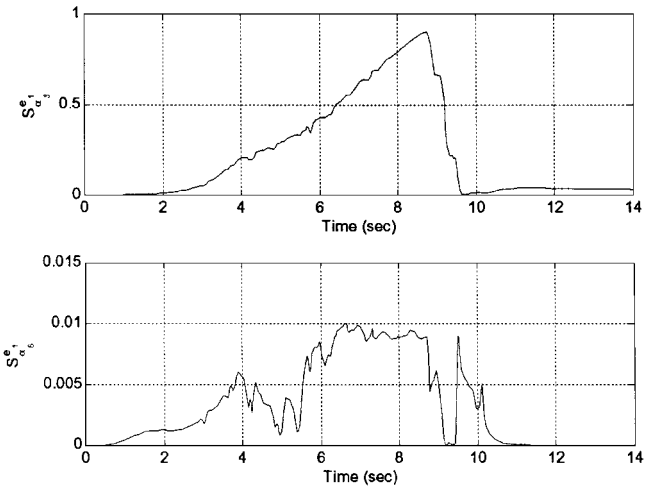

Fig. 12 Sensitivity of $\dot{x}$ trajectory error with respect to α_3 and α_6 for the least-robust operation.

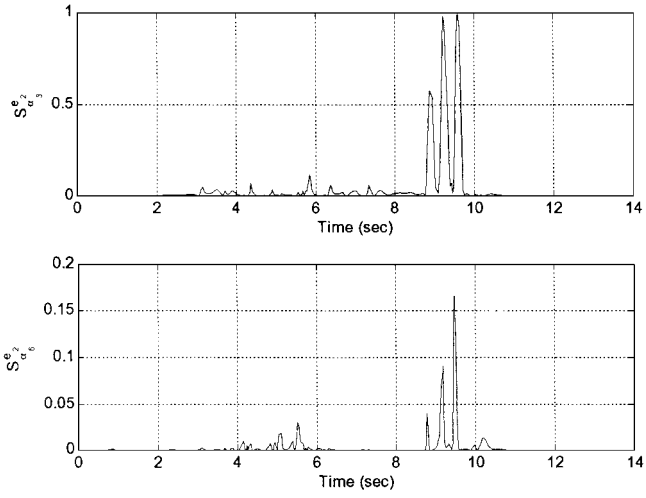

Fig. 13 Sensitivity of $\ddot{x}$ trajectory error with respect to α_3 and α_6 for the least-robust operation.

The parameters for $(\Delta\alpha_m)_1$ and $(\Delta\alpha_m)_2$ are given next:

$$[(\Delta\alpha_m)_1 \quad (\Delta\alpha_m)_2]^T = [1.00 \quad 1.00]^T$$

The fuzzy sets in Fig. 3 are represented using cosine membership functions (cosmf). The cosine membership function has the following definition:

$$\text{cosmf}(v; c, d) = \begin{cases} 1, & \text{if} \quad |v-c| > d \\ 0.5 * \cos[\pi (v-c)/d] + 0.5, & \text{if} \quad |v-c| \le d \end{cases}$$

where c is the center and d is the half-width of the membership function. The membership functions $\mu_{\Delta\alpha_1}(v) = \text{cosmf}(v; 0, 1)$ and $\mu_{\Delta\alpha_2}(v) = \text{cosmf}(v; 0, 1)$ are used for $\Delta\alpha_1$ and $\Delta\alpha_2$, respectively. Likewise, the membership function $\mu_{\Delta e_j}(v) = \text{cosmf}(v; 0, \Delta x_j)$ is used for Δe_j.

The sensitivities $S_{\alpha_1}^{e_j}$ and $S_{\alpha_2}^{e_j}$ are calculated numerically from Definition 6 using the cosine membership functions defined for $\Delta\alpha_1$, $\Delta\alpha_2$, and Δe_j. The values $\text{FRM}_{\min}$ and $\text{FRM}_{\max}$ are calculated in the following way:

1) Assuming ideal-case sensitivity, $S_{\alpha_1}^{e_j} \approx 0$ implies $\boldsymbol{P} \approx 0$. Therefore, $\text{FRM}_{\min} = \|\boldsymbol{P}\|_\infty \approx 0$.

2) Assuming worst-case sensitivity, $S_{\alpha_i}^{e_j} \approx 1/(1 - \mu_{\Delta\alpha_i})$ (for $i = 1, 2$). The parameter perturbations with the smallest magnitude that will be used to calculate $S_{\alpha_i}^{e_j}$ are $\Delta\alpha_1 = -0.01$ and $\Delta\alpha_2 = -0.01$. Therefore, $1 - \mu_{\Delta\alpha_1} = 1 - \text{cosmf}(-0.01; 0, 1) = 2.4672 \times 10^{-4}$ and $1 - \mu_{\Delta\alpha_2} = 1 - \text{cosmf}(-0.01; 0, 1) = 2.4672 \times 10^{-4}$.

For that reason, $S_{\alpha_1}^{e_j} k_{11} \approx -4.05$ and $S_{\alpha_1}^{e_j} k_{22} \approx -4.05$, where $k_{11} = -0.001$ and $k_{22} = -0.001$, and

$$\boldsymbol{P} = \begin{bmatrix} -8.10 & 0 & 0 & 0 \\ 0 & -8.10 & 0 & 0 \\ 0 & 0 & -8.10 & 0 \\ 0 & 0 & 0 & -8.10 \end{bmatrix}$$

implies that $\text{FRM}_{\max} = 8.10$. The value $h_{\max}$ is chosen to be

$$\int_{t_0}^{t_f} \left(\frac{\Delta \boldsymbol{x}}{4}\right)^T \left(\frac{\Delta \boldsymbol{x}}{4}\right) \mathrm{d}t = 0.95$$

where $\Delta \boldsymbol{x}$ is the maximum allowable deviation from the nominal trajectory, $t_0 = 0$ and $t_f = 14$ s.

The linguistic values of "very robust," "robust," "quite robust," "not quite robust," and "not robust" are assigned to FRM in the following manner: If $0.00 \le \text{FRM} \le 1.01$ then FRM is "very robust." If $1.01 < \text{FRM} \le 3.04$ then FRM is "robust." If $3.04 < \text{FRM} \le 5.07$ then FRM is "quite robust." If $5.07 < \text{FRM} \le 7.10$ then FRM is "not quite robust." If $7.10 < \text{FRM} \le 8.10$ then FRM is "not robust." The optimizations performed in this section are done using MATLAB's Optimization Toolbox with a tolerance of $1e{-}2$ for parameter perturbations and $1e{-}2$ for optimal function values.

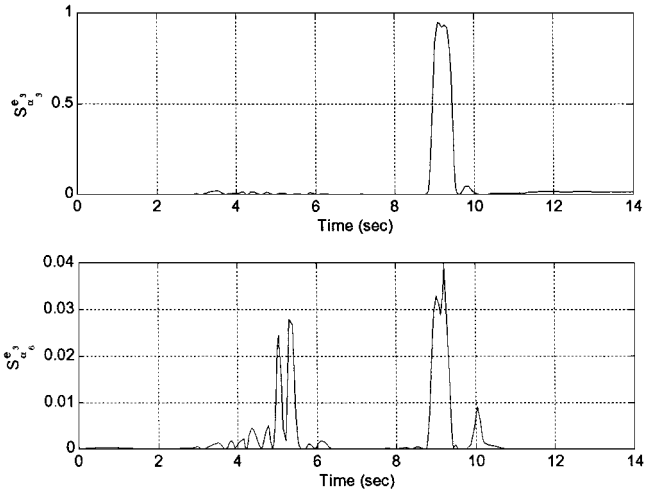

Fig. 14 Sensitivity of θ trajectory error with respect to α_3 and α_6 for the least-robust operation.

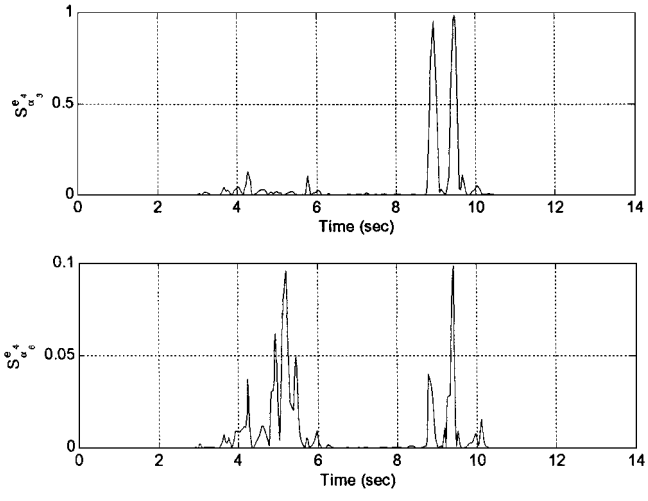

Fig. 15 Sensitivity of $\dot{\theta}$ trajectory error with respect to α_3 and α_6 for the least-robust operation.

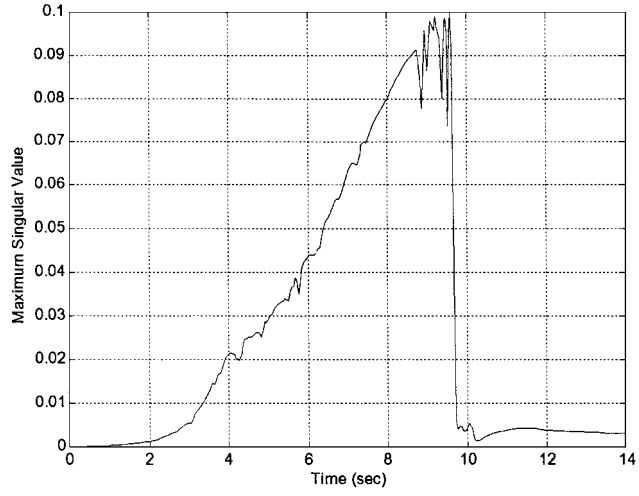

Fig. 16 Plot of $\bar{\sigma}(P, t)$ for the least-robust operation.

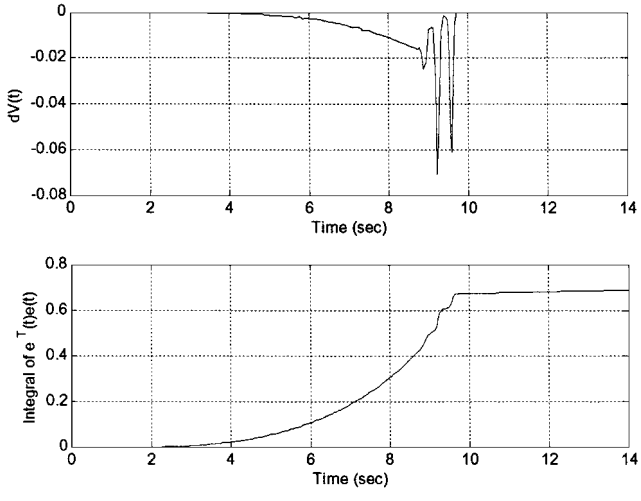

Fig. 17 Plots of d$V(t)$ and the integral of $e^T(t)e(t)$ for the least-robust operation.

The values of $\text{FRM}^*_{\max}$ and $h^*_{\max}$ are determined to be $\text{FRM}^*_{\max} = 0.14$ at $\Delta\alpha_1 = -1.00$, $\Delta\alpha_2 = -0.01$, and $h^*_{\max} = 0.69$ at $\Delta\alpha_1 = -1.00$, $\Delta\alpha_2 = -1.00$, where

$$h(\boldsymbol{e}) = \int_{t_0}^{t_f} \boldsymbol{e}^T(t)\boldsymbol{e}(t)\,\mathrm{d}t$$

is maximized over the space of parameter perturbations. Because $\text{FRM}^*_{\max}$ has a linguistic value "very robust" and $h^*_{\max} < h_{\max}$, the controller exhibits robust performance to the given range of parameter variations.

The least-robust perturbation is determined by maximizing the following performance criteria over the space of parameter perturbations:

$$\lambda_1 \int_{t_0}^{t_f} \boldsymbol{e}^T(t)\boldsymbol{e}(t)\,\mathrm{d}t + \lambda_2\,\text{FRM}, \qquad \lambda_1 = 0.5, \quad \lambda_2 = 0.5$$

The maximum value of

$$\frac{1}{2}\int_{t_0}^{t_f} \boldsymbol{e}^T(t)\boldsymbol{e}(t)\,\mathrm{d}t + \tfrac{1}{2}\text{FRM} = 0.40$$

occurred at $\Delta\alpha_1 = -1.00$, $\Delta\alpha_2 = -1.00$, where

$$\int_{t_0}^{t_f} \boldsymbol{e}^T(t)\boldsymbol{e}(t)\,\mathrm{d}t = 0.69$$

and FRM = 0.10. For the least-robust operation, Figs. 10–17 shows plots of the 1) trajectory errors, 2) the sensitivity functions of the trajectory errors with respect to parametric perturbations, 3) the maximum singular value of matrix $\boldsymbol{P}(t)$, and 4) d$V(\boldsymbol{e}, t)$ and

$$\int_{t_0}^{t} \boldsymbol{e}^T(t)\boldsymbol{e}(t)\,\mathrm{d}t$$

IV. Summary and Conclusions

An approximate method has been developed for analyzing the robust stability of nonlinear systems controlled using mode-to-mode fuzzy controllers. The type of stability considered in this paper is the Lyapunov stability of the nominal mode-to-mode trajectory in the presence of parametric or initial condition variations. This type of stability was chosen because it was desired to have the perturbed trajectories remain close to the nominal mode-to-mode trajectory that is assumed to have stability convergence from the equilibrium point of the start mode to the equilibrium point of the target mode of operation. Finally, a fuzzy robust measure is formulated quantitatively. The proposed method is illustrated via performing robust analysis of a hover mode to FF mode controller designed for a small-scale helicopter. The worst-case performance of the closed-loop system is determined by identifying the least-robust operation. The robust stability analysis of fuzzy controllers will assist in verifying the controller design and in demonstrating the controller performance under emergency maneuvering conditions.

References

[1]Farinwata, S. S., "Performance Assessment of Fuzzy Logic Control Systems via Stability and Robustness Measures," Ph.D. Dissertation, School of Electrical Engineering, Georgia Inst. of Technology, Atlanta, GA, Aug. 1993.

[2]Farinwata, S. S., and Vachtsevanos, G., "Robust Stability of Fuzzy Logic Control Systems," *Proceedings of the American Control Conference*, Vol. 5, American Automatic Control Council, New York, 1995, pp. 2267–2271.

[3]Teo, K. L., Goh, C. J., and Wong, K. H., *A Unified Computational Approach to Optimal Control Problems*, Wiley, New York, 1991, pp. 213–234.

[4]Hargraves, C. R., and Paris, S. W., "Direct Trajectory Optimization Using Nonlinear Programming and Collocation," *Journal of Guidance, Control, and Dynamics*, Vol. 10, No. 4, 1987, pp. 332–342.

[5]Vachtsevanos, G., Farinwata, S. S., and Pirovolou, D. K., "Fuzzy Logic Control of an Automotive Engine," *IEEE Control Systems Magazine*, Vol. 13, No. 3, 1993, pp. 62–68.

[6]Kang, H., and Vachtsevanos, G., "Nonlinear Fuzzy Control Based on the Vector Field of the Phase Portrait Assignment Algorithm," *Proceedings of the American Control Conference*, 1990, pp. 1479–1484.

[7]Kang, H., "Stability and Control of Fuzzy Dynamic Systems via Cell-State Transitions in Fuzzy Hypercubes," *IEEE Transactions on Fuzzy Systems*, Vol. 1, No. 4, 1993, pp. 267–279.

[8]Slotine, J. E., and Li, W., *Applied Nonlinear Control*, Prentice–Hall, New Jersey, 1991, pp. 108, 109.